EISEVIED

Contents lists available at ScienceDirect

Inorganic Chemistry Communications

journal homepage: www.elsevier.com/locate/inoche



Short communication

Single-molecule magnet behavior in a tetranuclear cyano-bridged Fe^{III}₂Ni^{II}₂ cluster



Cheng-Qi Jiao, Wen-Jing Jiang, Wen Wen, Yi Ren, Jia-Liang Wang, Tao Liu*, Cheng He

State Key Laboratory of Fine Chemicals, Dalian University of Technology, Dalian 116024, China

ARTICLE INFO

Article history:
Received 24 September 2016
Received in revised form 19 October 2016
Accepted 21 October 2016
Available online 24 October 2016

Keywords: Cyanide Tetranuclear structure Ferromagnetic interactions Single-molecule magnets

ABSTRACT

A tetranuclear cyanide-bridged $\text{Fe}^{\text{III}}_2\text{Ni}^{\text{II}}_2$ cluster $[\text{Fe}^{\text{III}}(\text{Tp})(\text{CN})_3]_2\text{Ni}^{\text{II}}_2(4,4'\text{-dibromo-2},2'\text{-bpy})_4\cdot2\text{ClO}_4(1)$ (Tp = hydrotris(pyrazolyl)borate) was synthesized. Magnetic measurements indicated that this compound displayed single-molecule magnet behavior with the pre-exponential factor of $\tau_0 = 1.79(8) \times 10^{-10}$ s and the relaxation energy barrier of $\Delta/k_B = 65.1(9)$ K.

© 2016 Elsevier B.V. All rights reserved.

Since the most celebrated example of single-molecule magnets (SMMs) was discovered in the oxo-manganese family [1,2], SMMs have attracted increasing interest because they exhibit the slow magnetic relaxation as well as with potential applications in high-density information storage and quantum computation [3-5]. Therefore, the rational design and synthesis of the SMMs has become a particularly important subject. Recently, considerable effort has been devoted to utilizing metallocyanate building blocks as multidentate ligands and linkers for the preparation of high-spin anisotropic clusters, and some of them indicate the slow relaxation of SMMs [6–12]. For cyanide-bridged systems, the topological structures and the nature of the magnetic exchange interactions in the resulting clusters can be well controlled and predicted [7]. Therefore, metallocyanate building blocks have been extensively employed. Among them, a number of cyanide-bridged SMMs derived from the tricyanide precursors fac- $[Fe(Tp^R)(CN)_3]^-$ with tri-, tetra-, and octanuclear structures have been reported during the last decade [10,13-19]. Among the various structures, a few reports have been devoted to the structures and magnetic studies of heterobimetallic tetranuclear square clusters that incorporated anisotropic Ni^{II} ion, and some of them display single-molecule magnet behavior [20–27]. Generally, the interactions between low-spin Fe^{III} and highspin Ni^{II} are ferromagnetic, preferring a high-spin state that benefits SMM behavior. In our previous work, using the building block [Fe(Tp)(CN)₃]⁻ and 1, 10-phen ligand, a tetranuclear cyanide-bridged Fe₂Ni₂ compound exhibiting SMM behavior, [Fe^{III}(Tp)(CN)₃]₂Ni^{II}₂(1, 10-phenanthroline)₄·2ClO₄·2H₂O has been reported [27]. As an expansion of this work, we replaced 1, 10-phen ligand with much larger steric hindrance ancillary ligand 4, 4′-dibromo-2, 2′-bpy, and this change no influence on the construction of the tetranuclear cluster. Furthermore, the enhancement in the steric effect is one of the possible approaches to distort the Ni^{II} coordination sphere and decreases the intermolecular interaction, and then the energy barrier of the ${\rm Fe^{II}}_2{\rm Ni^{II}}_2$ compound may also be systematically tuned. With this strategy, a cyano-bridged tetranuclear ${\rm [Fe^{III}(Tp)(CN)_3]_2Ni^{II}}_2(4,4'$ -dibromo-2, 2'-bpy)₄·2ClO₄ (1) cluster was prepared.

Compound 1 was synthesized by a diffusion method and obtained as orange block crystals [28]. X-ray crystallographic analysis revealed that compound 1 crystallizes in the triclinic space group P^{-1} and exhibits a tetranuclear square structure [29] (Table S1). Within the square (Fig. 1a), each [Fe^{III}(Tp)(CN)₃]⁻ fragment is alternatively connected with two [Ni(4, 4'-dibromo-2, 2'-bpy)₂]²⁺ units through two of its three cyano groups, forming a $\{Fe_2(\mu-CN)_4Ni_2\}$ tetranuclear square structure. Each Fe^{III} center adopts a slightly distorted octahedral configuration consisting of three cyanide carbon atoms and three nitrogen atoms of Tp^- anion. The Fe— $C_{(cvanide)}$ [1.896(9)–1.948(13) Å] and Fe— $N_{(Tp)}$ [1.975(7)–2.006(9) Å] bond lengths are in good agreement with those observed previously in the related low-spin (LS) Fe^{III} compounds [13-19] (Table S2). The Fe—C≡N bond angles in the range of 175.1(8)– 178.8(11)°, departing slightly from linearity. In the [Ni(4, 4'-dibromo-2, 2'-bpy)₂|²⁺ unit, each Ni^{II} ion is also octahedral coordination. Four N atoms comes from two bidentate 4, 4'-dibromo-2, 2'-bpy ligands, the remaining coordination sites of each six-coordinated Ni^{II} ion are occupied by the bridging cyanide building blocks. The Ni—N distances [2.042(7)–2.117(8) Å] are comparable with related high-spin (HS) Ni^{II} compounds previously reported [20–27]. The Ni—N≡C bond angles deviate significantly from linearity with the angles of $152.5(8)-166.4(7)^{\circ}$. The neighboring molecules are linked together through $C{-\!\!\!\!-} H{\cdot}{\cdot}{\cdot}\pi$ and

^{*} Corresponding author. E-mail address: liutao@dlut.edu.cn (T. Liu).

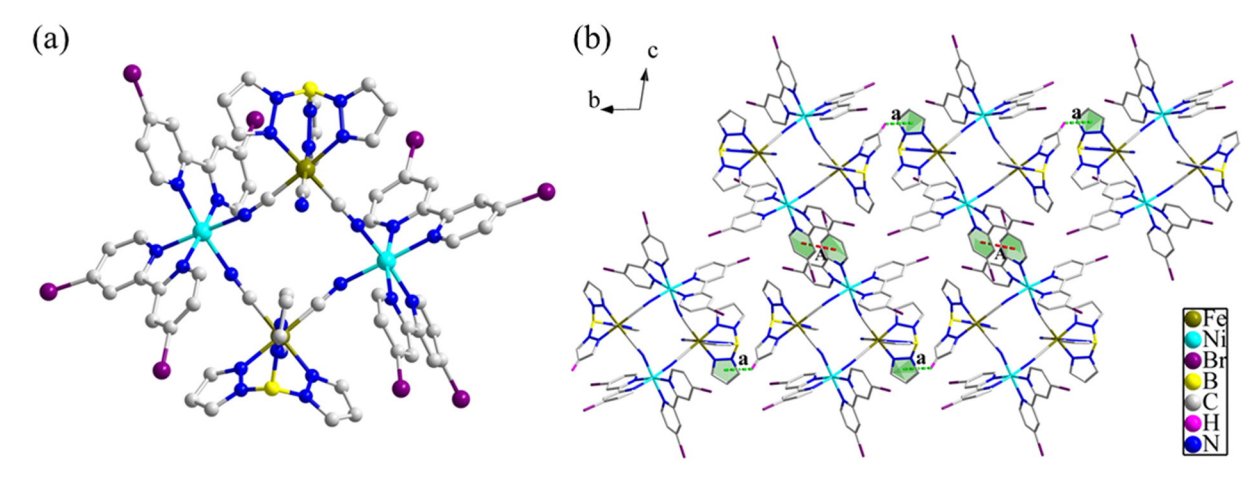


Fig. 1. (a) Crystal structures of **1**. The hydrogen atoms and water molecules are omitted for clarity Atomic scheme: Fe, bright green; Ni, turquoise; C, gray; N, blue; B, yellow; Cl, violet; O, red. (b) Packing diagrams for **1** illustrating close $\pi \cdots \pi$ (A: distance = 4.156 Å) and C—H $\cdots \pi$ (a: distance = 3.226 Å) contacts in the *bc* plane. (For interpretation of the references to colour in this figure legend, the reader is referred to the web version of this article.)

 $\pi\cdots\pi$ interactions, resulting in a 2D supramolecular layer structure (Fig. 1b). The shortest intramolecular Fe \cdots Ni, Fe \cdots Fe and Ni \cdots Ni distances are 4.578(4), 6.436(2) and 6.722(6) Å respectively, while the nearest intermolecular Fe \cdots Ni, Fe \cdots Fe and Ni \cdots Ni distances are 9.628(3), 7.904(7) and 9.517(6) Å respectively, indicating that the intermolecular magnetic interactions are very weak.

The magnetic susceptibility data of **1** were measured at 1000 Oe in the temperature range of 2–300 K (Fig. 2a). The χT value is 3.71 cm³⁻ mol⁻¹ K at 300 K, which is in agreement with the spin-only value of 3.69–4.12 cm³ mol⁻¹ K expected for two uncoupled LS Fe^{III} (S=1/2, g=2.6-2.8) and two Ni^{II} (S=1, g=2.2-2.3). As the temperature is lowered, the χT value remains essentially constant up to 75 K and abruptly increases to reach the maximum value of 11.05 cm³ mol⁻¹ K

at 6.1 K. The overall magnetic behavior indicates the intramolecular ferromagnetic interactions between Fe^{III} and Ni^{II} ions. The maximum value of 11.05 cm³ mol $^{-1}$ K is larger than the theoretical value ($\chi T=0.125g^2S(S+1)=6.0~{\rm cm}^3~{\rm mol}^{-1}$ K, g=2.0) for the magnetically isolated tetranuclear compound with S=3 ground state, which is aroused by the intermolecular ferromagnetic interactions and deviated g value. Upon further lowing, the χT value decreases to 8.94 cm³ mol $^{-1}$ K at 2.0 K. Such behavior may be due to the zero-field splitting and/or intermolecular interactions. The magnetic susceptibility data for 1 are fitted by the Curie–Weiss law in the temperature range of 2–300 K, give $C=3.66(1)~{\rm cm}^3~{\rm mol}^{-1}$ K and $\theta=7.71(4)$ K (Fig. S1). The positive Weiss temperature further demonstrates the ferromagnetic coupling interactions between the paramagnetic centers. The magnetic behavior

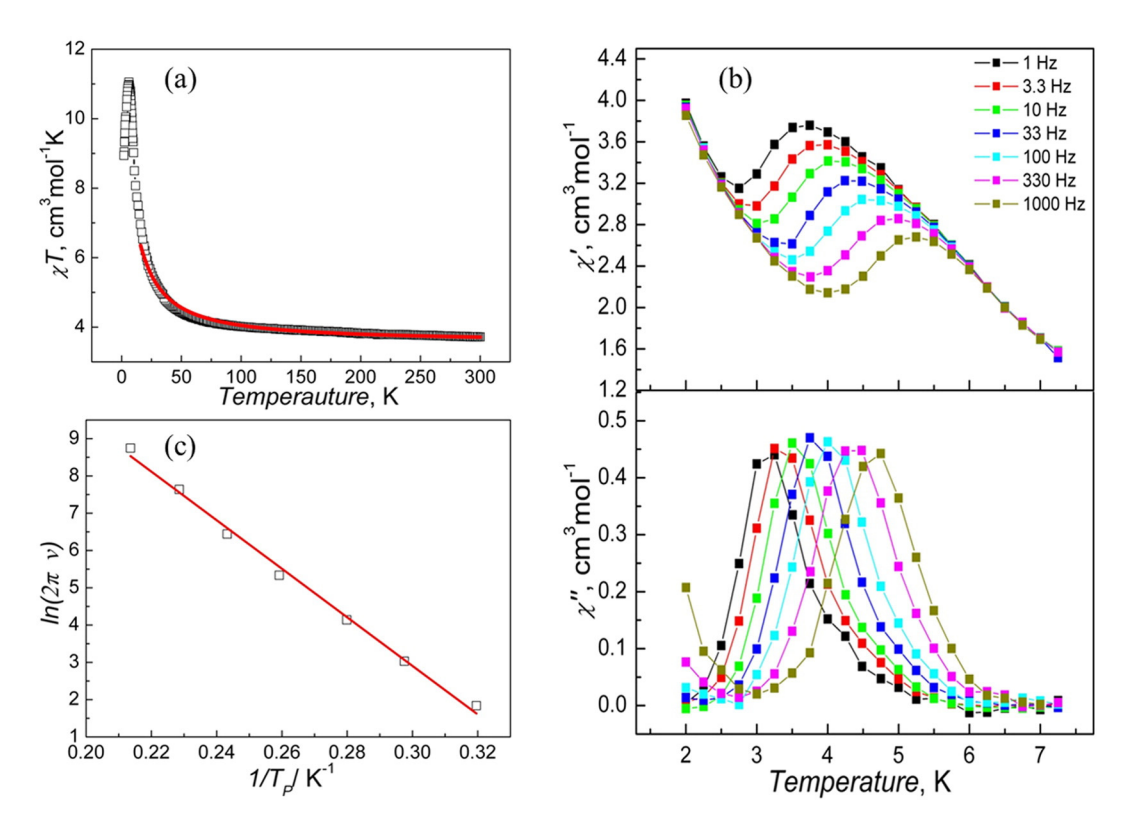


Fig. 2. (a) Temperature-dependent magnetic susceptibilities of **1** in the temperature range of 2–300 K under an applied field of 1000 Oe. The red solid line represents the best fit of the experimental results. (b) Temperature dependence of the real part and the imaginary part of the ac susceptibility of **1** in a zero dc field and a 3.5 Oe ac field. (c) The plot of $\ln(2\pi v)$ versus T_P^{-1} of 1, where v is the frequency and T_P is the peak temperature of χ'' . The solid line represents the least-squares fit of the experimental data to the Arrhenius equation. (For interpretation of the references to colour in this figure legend, the reader is referred to the web version of this article.)

Download English Version:

https://daneshyari.com/en/article/5151317

Download Persian Version:

https://daneshyari.com/article/5151317

<u>Daneshyari.com</u>